

Electronic Supporting Information for:

The effects of cononsolvents on the synthesis of responsive particles via polymerisation-induced thermal self-assembly.

Marissa D. Morales-Moctezuma and Sebastian G. Spain*

Polymer and Biomaterials Chemistry Laboratories, Department of Chemistry, University of Sheffield, Sheffield S3 7HF, UK.

E-mail: s.g.spain@sheffield.ac.uk

Contents

Characterisation of poly(acrylic acid) macroCTAs.....	S2
SEC Chromatograms.....	S2
¹ H NMR Spectra.....	S2
Summary of characterisation data for poly(acrylic acid) macroCTAs	S4
DLS correlation functions for pAA- <i>b</i> -pNIPAM/BIS nanogels	S5
Summary of characterisation data for pAA- <i>b</i> -pNIPAM/BIS nanogels.....	S6
Number particle size distribution of pAA ₄₅ - <i>b</i> -pNIPAM ₁₇₅ /BIS ₃ nanogels.....	S6
Characterisation of pAA ₄₅ - <i>b</i> -pNIPAM ₈₇ /BIS ₃ nanogels	S7
Characterisation of pAA ₄₅ - <i>b</i> -pNIPAM ₂₆₂ /BIS ₃ nanogels.....	S8
Synthesis of pNIPAM <i>via</i> ethanolic RAFT solution polymerisation.....	S9
Cloud point measurements of linear pNIPAM in water/EtOH mixtures	S9
Synthesis of pNIPAM <i>via</i> free radical precipitation polymerisation.....	S10
SEC of pNIPAM homopolymers synthesised in cononsolvents	S10
Determination of the volume phase transition temperature (VPTT) of nanogels.....	S11
Summary of data for pAA ₃₄ - <i>b</i> -pNIPAM _x block copolymers	S12
Cloud point measurements of pAA ₃₄ - <i>b</i> -pNIPAM ₁₈₄ diblock copolymers synthesised in water and water/EtOH mixtures	S12
¹ H NMR spectra of pNIPAM homopolymers synthesised in cononsolvents.....	S13
Notes and references	S14

Characterisation of poly(acrylic acid) macroCTAs

SEC Chromatograms

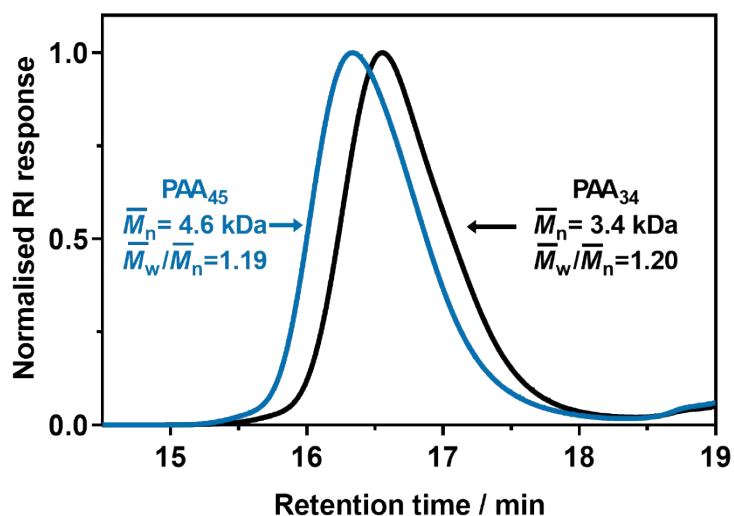


Figure S1. SEC chromatograms for poly(acrylic acid) macroCTAs synthesised by RAFT-mediated polymerisation in ethanol. SEC conditions: THF containing 4% w/v AcOH and 0.025% w/v BHT, calibrated with narrow PMMA standards. Samples were methylated with trimethylsilyl diazomethane before analysis.

¹H NMR Spectra

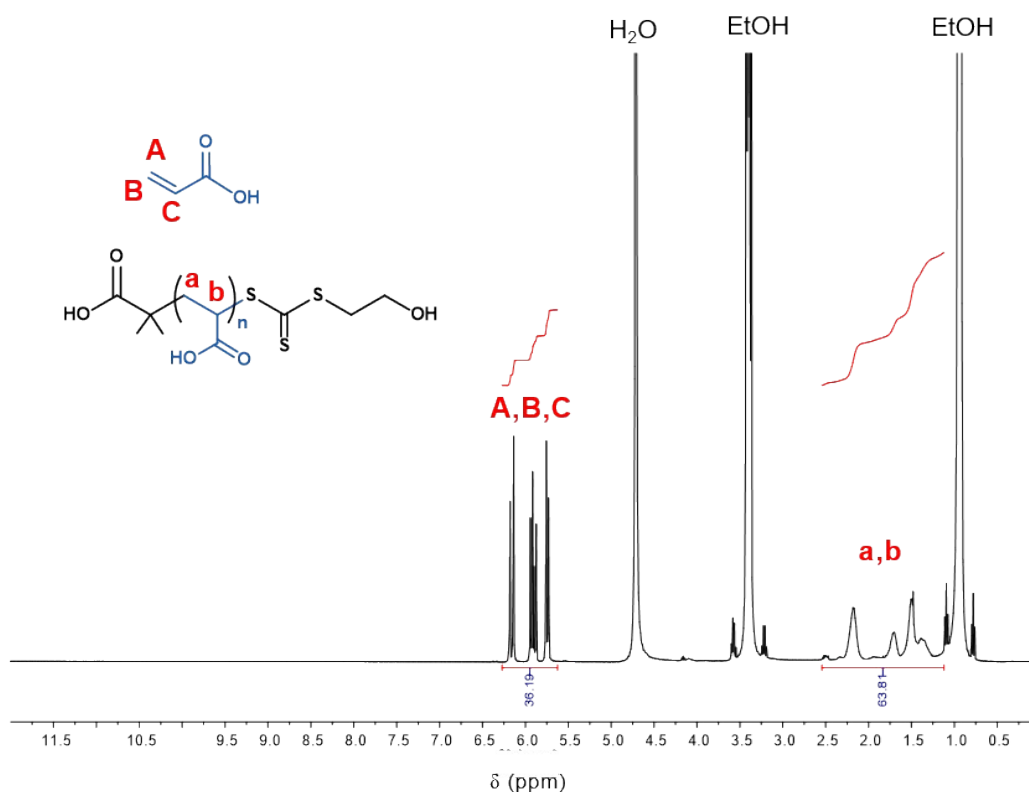


Figure S2. ¹H NMR spectrum of pAA₃₄ macro-CTA before purification for determination of monomer conversion.

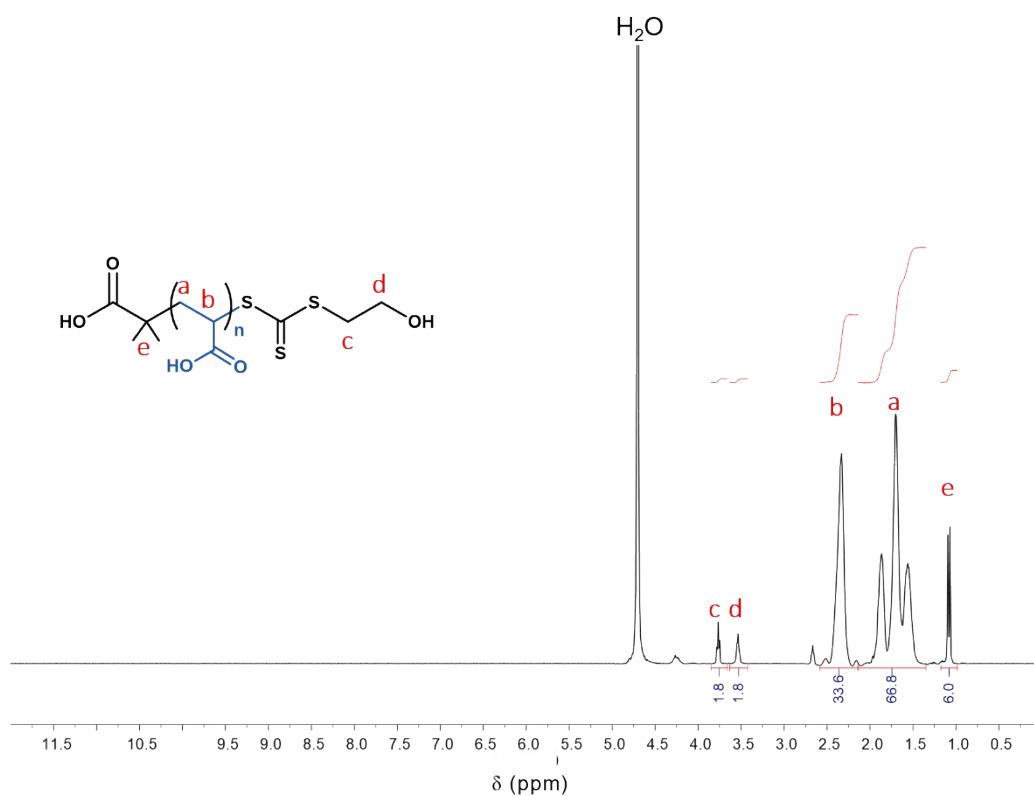


Figure S3. ¹H NMR spectrum of pAA₃₄ macro-CTA after purification for determination of DP_n .

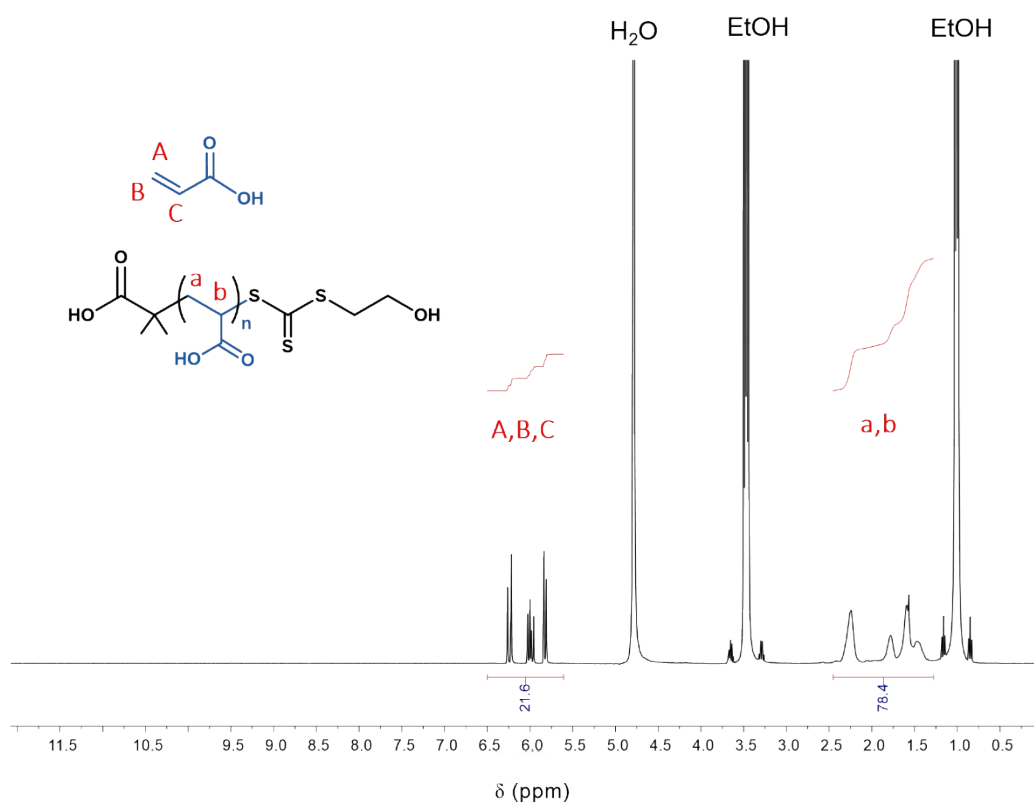


Figure S4. ¹H NMR spectrum of pAA₄₅ macro-CTA before purification for determination of monomer conversion.

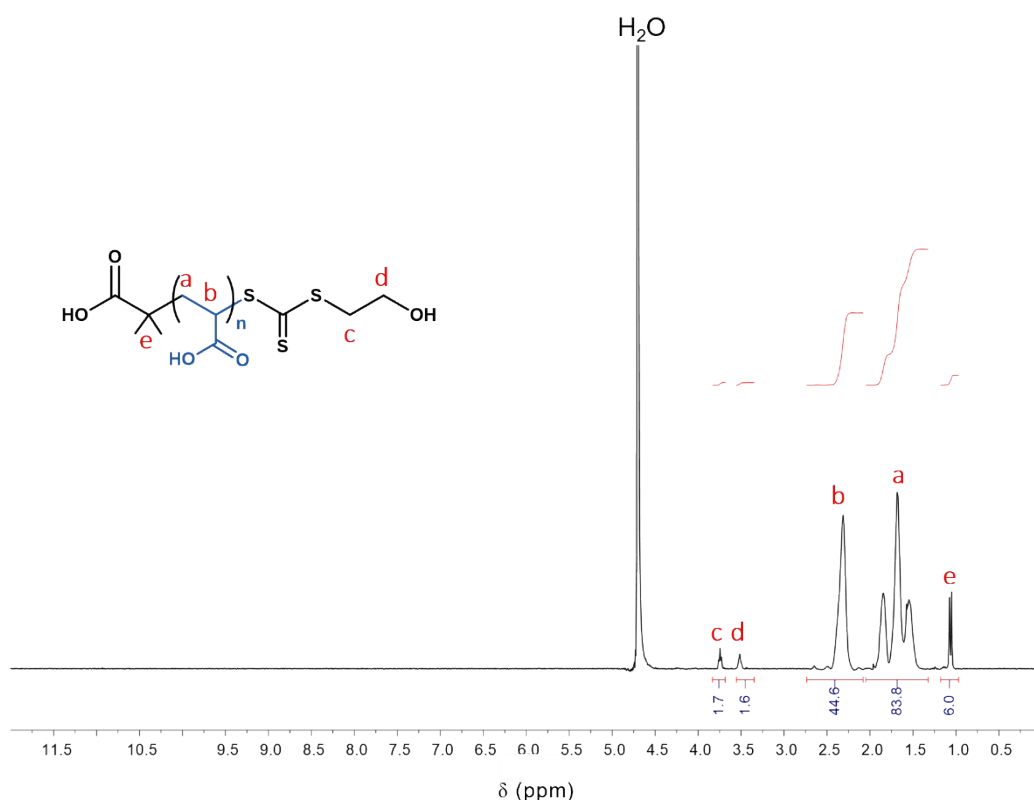


Figure S5. ^1H NMR spectrum of pAA₄₅ macro-CTA after purification for determination of DP_n .

Summary of characterisation data for poly(acrylic acid) macroCTAs

Table S1. Summary of the data for pAA macroCTAs.

[AA]/[HEMP] ^a	[HEMP]/[AIBN] ^a	Conversion ^b / %	$DP_{n,theo}$ ^c	$DP_{n,NMR}$ ^d	$M_{n,theo}$ ^e / kDa	$M_{n,SEC}$ ^f / kDa	M_w/M_n ^f
61	10	64	39	34	3.2	3.4	1.20
60	5	78	47	45	4.1	4.6	1.19

^aGeneral reaction conditions: solids content 25% w/w in EtOH and 70 °C. ^bDetermined by ^1H NMR spectroscopy using the ratio of the sum of vinyl proton integrals and the repeating monomer units. ^cCalculated using $DP_{n,theo} = [\text{AA}]/[\text{HEMP}] \times \text{conversion}$. ^dCalculated from the end-group analysis using the proton signals corresponding only to the R-group of the CTA ($2 \times \text{CH}_3$) and the protons from the polymer backbone by ^1H NMR spectroscopy. ^eCalculated using $M_{n,theo} = M_e + (DP_n \times M_{MA})$ where M_e is the molecular weight of the end groups and M_{MA} is the molecular weight of the esterified AA repeating unit. ^fDetermined by SEC after methylation of the purified pAA macro-CTAs. (GPC: THF 4% acetic acid, 0.025% BHT, calibrated with near-monodisperse pMMA standards).

DLS correlation functions for pAA-*b*-pNIPAM/BIS nanogels

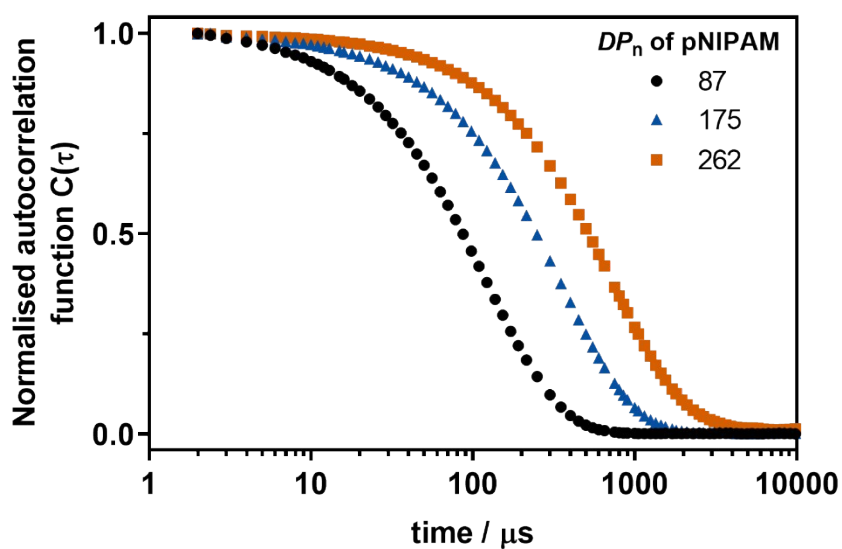


Figure S6. DLS Correlation functions for pAA₄₅-*b*-pNIPAM_x/BIS₃ nanogels synthesised in water, where x= 87, 175 and 262.

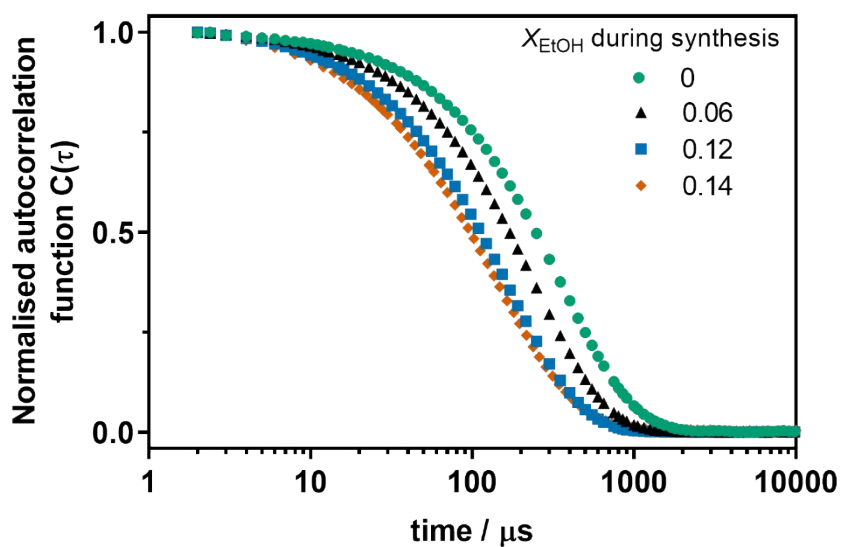


Figure S7. DLS Correlation functions for pAA₄₅-*b*-pNIPAM₁₇₅/BIS₃ nanogels synthesised in water/EtOH mixtures.

Summary of characterisation data for pAA-*b*-pNIPAM/BIS nanogels

Table S2. Data for the synthesis of pAA₄₅-*b*-pNIPAM_x/BIS₃ nanogels by RAFT dispersion polymerisation in water/ethanol mixtures

Target composition [pAA ₄₅]:[NIPAM]:[BIS] ^a	X_{EtOH} ^b	Conversion ^c / %	$DP_{n,\text{theo}}$ ^d	$M_{n,\text{theo}}$ ^e / kg mol ⁻¹	$D_h \pm \text{S.D.} / \text{nm}^f$ (PDI)	ζ -potential $\pm \text{S.D.}^g$ / mV
[1]:[87]:[3]	0.06	99	87	13.8	56 \pm 19 (0.11)	-29.7 \pm 3.9
[1]:[87]:[3]	0.12	79	69	11.8	55 \pm 25 (0.21)	-32.6 \pm 5.5
[1]:[87]:[3]	0.14	100	87	13.8	67 \pm 34 (0.25)	-29.4 \pm 5.3
[1]:[262]:[3]	0.12	86	226	29.5	203 \pm 67 (0.11)	-17.6 \pm 1.4

^aGeneral reaction conditions: Targeted [pAA₄₅]/[ACVA]=5, solids content 10% w/w, 70 °C for 18 h. ^bMole fraction of ethanol used during nanogel synthesis.

^cGravimetric determination by moisture analysis of solids content against predicted solids content. ^dFor an equivalent diblock synthesised without crosslinker, estimated from [NIPAM]/[pAA₄₅] \times conversion. ^eCalculated using $M_{n,\text{theo}} = M_e + nM_{\text{AA}} + xM_{\text{NIPAM}} + yM_{\text{BIS}}$, where M_e is the molecular weight of the CTA end groups, n, x and y are the DP_n of pAA, pNIPAM, and BIS respectively. ^fDLS data obtained from 0.1% w/v nanogels dispersions in DI water at pH 7 and 25 °C. ^gAverage zeta-potential and the standard deviation of five run measurements for 0.1% w/v nanogels dispersions in DI water with 1 mM KCl at pH 7 and 25 °C.

Number particle size distribution of pAA₄₅-*b*-pNIPAM₁₇₅/BIS₃ nanogels

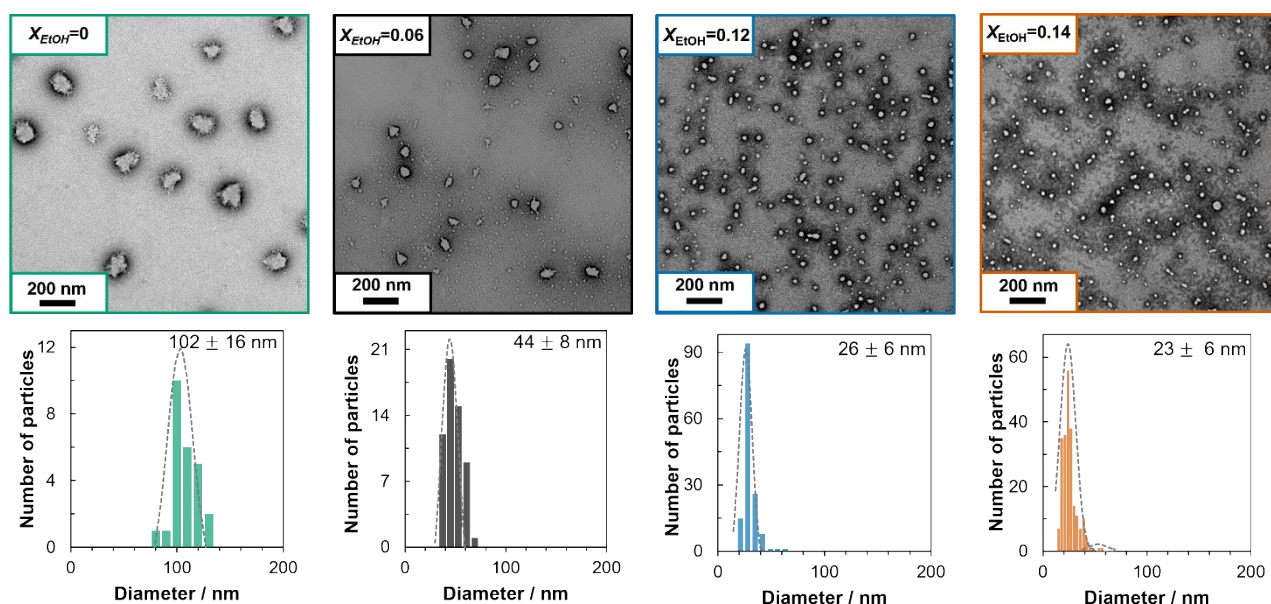


Figure S8. Transmission electron micrographs with their number particle size distributions of pAA₄₅-*b*-pNIPAM₈₇/BIS₃ nanogels synthesised in water/EtOH mixtures

Characterisation of pAA₄₅-*b*-pNIPAM₈₇/BIS₃ nanogels

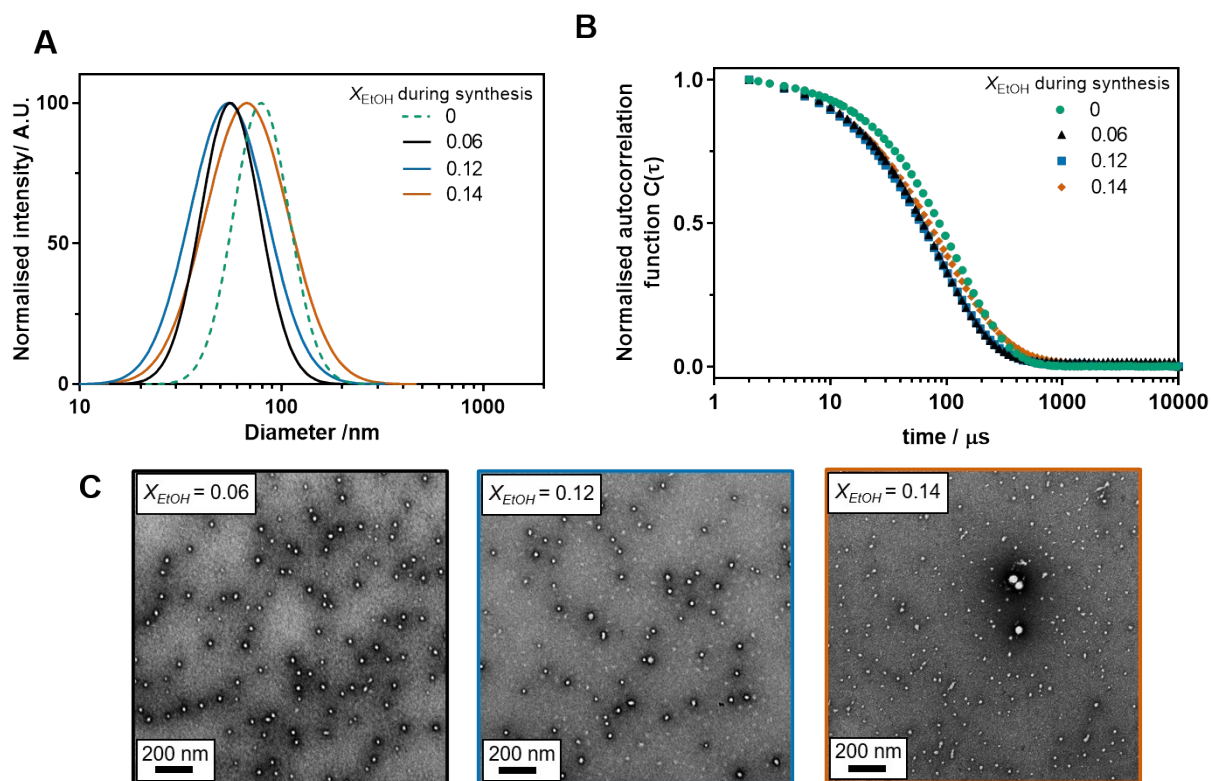


Figure S9. Characterisation of pAA₄₅-*b*-pNIPAM₈₇/BIS₃ nanogels synthesised in water/EtOH mixtures (a) Intensity average lognormal size distribution curves and (b) their respective autocorrelation functions with time from dynamic light scattering. (c) Transmission electron micrographs. DLS and TEM samples were prepared from 0.1% w/v nanogel dispersions in water at pH 7 at 25 °C. TEM samples were stained with phosphotungstic acid (0.75% w/v, pH 7).

Characterisation of pAA₄₅-*b*-pNIPAM₂₆₂/BIS₃ nanogels

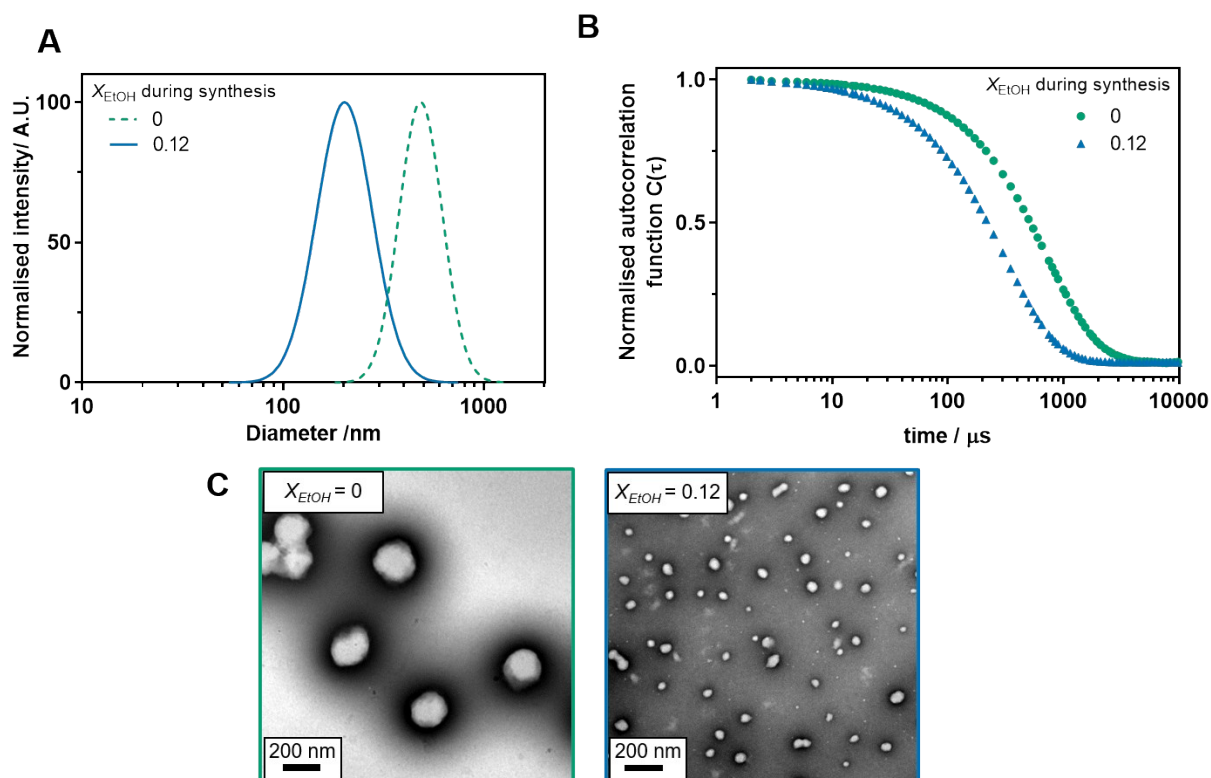


Figure S10. Characterisation of pAA₄₅-*b*-pNIPAM₂₆₂/BIS₃ nanogels synthesised in water/EtOH mixtures (a) Intensity average lognormal size distribution curves and (b) their respective autocorrelation functions with time from dynamic light scattering. (c) Transmission electron micrographs. DLS and TEM samples were prepared from 0.1% w/v nanogel dispersions in water at pH 7 at 25 °C. TEM samples were stained with phosphotungstic acid (0.75% w/v, pH 7).

Synthesis of pNIPAM *via* ethanolic RAFT solution polymerisation.

A mixture of NIPAM (3.01 g, 26.59 mmol), HEMP (0.06 g, 0.27 mmol), AIBN (0.008 g, 0.08 mmol) and ethanol (to give a 25% w/w solids solution) was purged thoroughly with N₂ for 30 minutes. The flask was then placed onto a DrySyn® heating block preheated to 70 °C and left to react for 240 minutes. The reaction was quenched by removing the flask from the heat source and opened to air. NIPAM conversion (98%) was calculated by ¹H NMR spectroscopy. The product was recovered by precipitation into hexane (400 mL). The product was then dissolved in water and purified by dialysis against water and freeze-drying to give a pale-yellow solid. PNIPAM₉₈ $\bar{M}_n = 9.0$ kDa, $\bar{M}_w/\bar{M}_n = 1.31$. PNIPAM₁₉₀: conversion (95%) $\bar{M}_n = 19.6$ kDa, $\bar{M}_w/\bar{M}_n = 1.35$; δ H (400 MHz; CDCl₃, 25 °C) (ppm): 3.42 (br. s, H, -NCH), 2.67 (s, 2H, -CH₂SC), 2.48-1.95 (br. d, 1H, -CH-), 1.95-1.46 (br. t, 2H, -CH₂-), 1.11 (br. s, 6H, -CH(CH₃)₂).

Cloud point measurements of linear pNIPAM in water/EtOH mixtures

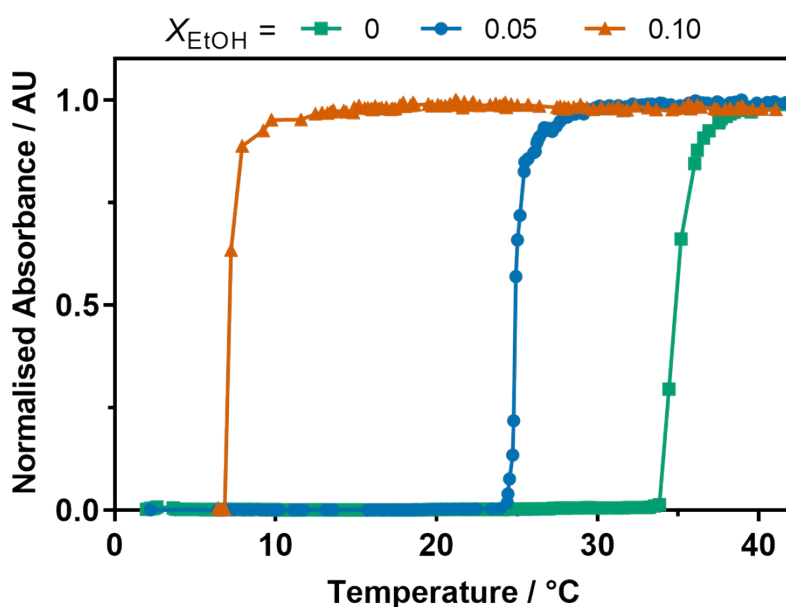


Figure S11. Cloud point curves of pNIPAM₉₈ in different X_{EtOH} fractions. Polymers were synthesised *via* RAFT ethanolic polymerisation. The cloud points were determined from the inflection point of the normalised absorbance curve at 550 nm at a heating rate of 0.12 °C min⁻¹

Synthesis of pNIPAM *via* free radical precipitation polymerisation.

NIPAM (0.5 g, 4.4 mmol) was dissolved in the corresponding water-ethanol cononsolvent mixture and degassed with N_2 for 30 minutes. Ammonium persulfate (0.32 mL, 69.3 mM) in water previously degassed was added *via* syringe into each of the NIPAM solutions to give a 10% w/w solids solution. The target mole fractions of ethanol and water were $X_e=0$, $X_e=0.05$, $X_e=0.10$ and $X_e=0.15$. Solutions were immersed into an oil bath preheated to 70 °C and left to react overnight. NIPAM monomer conversion (100 %) was estimated by 1H NMR spectroscopy. The crude product was dialysed against DI water to exchange ethanol to water. For further characterisation, the polymers were freeze-dried to give white solids. δH (400 MHz, D_2O , 25 °C): 3.81 (br. d, H, -NCH), 2.30-1.79 (br. d, 1H, -CH-), 1.79-1.27 (br. t, 2H, -CH₂-), 1.27-0.24 (br. s, 6H, -CH(CH₃)₂).

SEC of pNIPAM homopolymers synthesised in cononsolvents

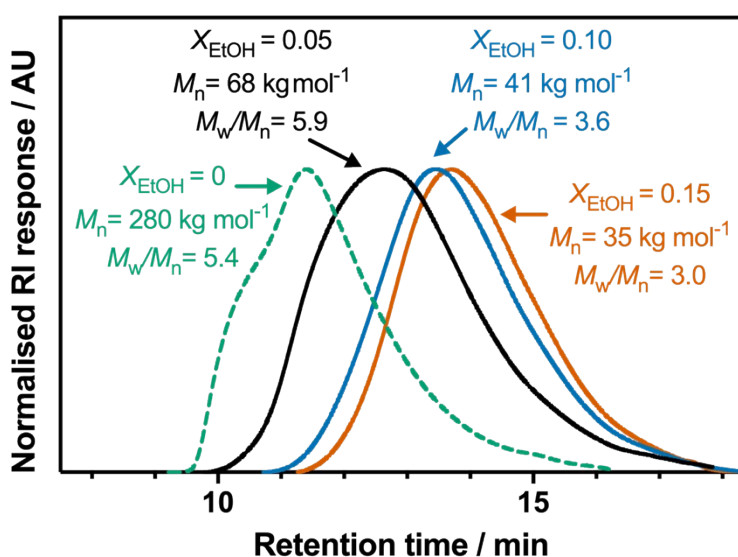


Figure S12. SEC chromatograms of pNIPAM homopolymers synthesised by precipitation polymerisation in different water and water/EtOH mixtures. SEC was performed in DMF (0.1% w/v LiBr) against pMMA standards.

Determination of the volume phase transition temperature (VPTT) of nanogels

The experimental D_h data was fitted with a Boltzmann sigmoidal model using a least squares regression to assist in the determination of the VPTT of the aqueous nanogel dispersions. The fit using sigmoidal models have previously been reported to determine the VPTT indicating a good approximation to experimental data.^{1,2} Herein, Equation S1 relates the hydrodynamic size (D_h) at a specific temperature (T), where D_t and D_b are respectively the swollen (“top” temperature at 12.5 °C) and shrunken (“bottom” temperature 60 °C) hydrodynamic diameters, ω is the halfway point between the swollen and shrunken state (i.e. VPTT) and σ is the steepness of the curve (i.e. the sharpness around the phase transition).

$$D_h = D_t + \frac{D_t - D_b}{1 + e^{\left(\frac{\omega - T}{\sigma}\right)}} \quad \text{Equation S1}$$

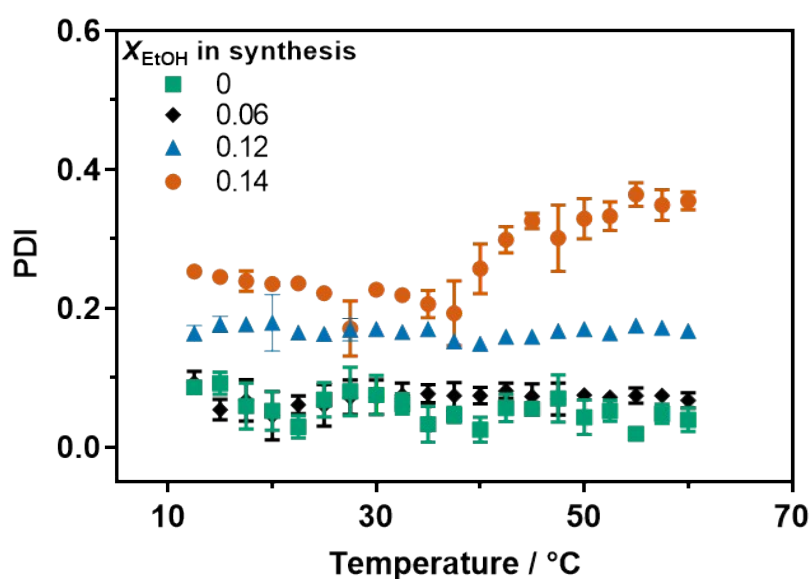


Figure S13. Variable temperature PDI data for pAA₄₅-*b*-(pNIPAM₁₇₅/BIS₃) nanogels synthesised in water and water/EtOH mixtures as obtained by DLS.

Summary of data for pAA₃₄-*b*-pNIPAM_x block copolymers

Table S3. Summary of data for pAA₃₇-*b*-pNIPAM_x block copolymers

Targeted pNIPAM DP_n (x) ^a	X_{EtOH} ^b	Conversion ^c / %	$DP_{n,\text{theo}}$ ^d	Cloud point (T_c) ^e / °C	$D_h \pm \text{S.D.} / \text{nm}$ (PDI) ^f
92	0	>99	92	43	ill-defined
92	0.06	99	92	43	139 ± 57 (0.17)
92	0.11	99	91	45	178 ± 50 (0.08)
92	0.14	>99	92	47	153 ± 55 (0.13)
184	0	>99	184	34	49 ± 12 (0.06)
184	0.06	>99	184	36	63 ± 13 (0.04)
184	0.12	>99	184	39	93 ± 44 (0.22)
184	0.15	99	182	39	140 ± 56 (0.16)
280	0	>99	280	34	60 ± 12 (0.04)
280	0.06	99	277	34	63 ± 19 (0.09)
280	0.12	99	277	35	92 ± 36 (0.15)
280	0.15	99	277	36	141 ± 56 (0.16)

^aGeneral reaction conditions: Targeted [pAA₃₄]/[ACVA]=5, solids content 10% w/w, 70 °C for 18 h. ^bMole fraction of ethanol used during nanogel synthesis. ^cGravimetric determination by moisture analysis of solids content against predicted solids content. ^dEstimated from [NIPAM]/[pAA₃₄] \times conversion. ^eCloud points were estimated from the inflection point of the normalised absorbance curve of 1% w/v dispersions in water at 550 nm at a heating rate of 0.12 °C min⁻¹. ^fDLS data obtained from 0.1% w/v dispersions in DI water at pH 7 and 50 °C.

Cloud point measurements of pAA₃₄-*b*-pNIPAM₁₈₄ diblock copolymers synthesised in water and water/EtOH mixtures

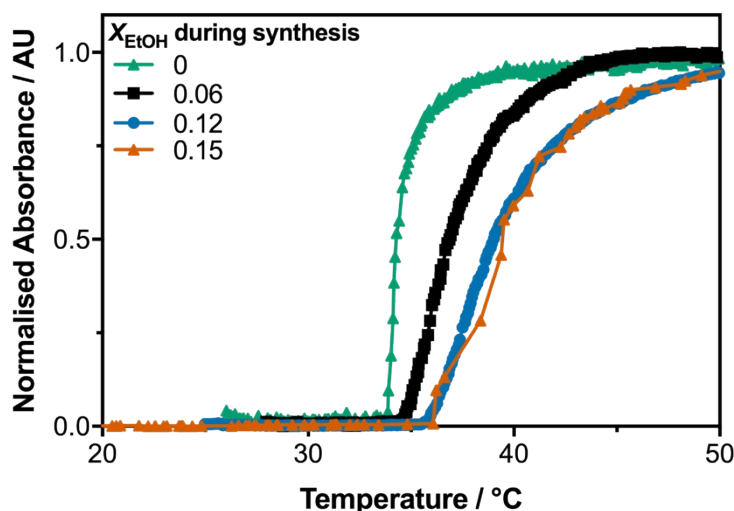


Figure S14. Turbidimetry experiments of purified pAA₃₄-*b*-pNIPAM₁₈₄ diblock copolymers at pH 7 in water.

^1H NMR spectra of pNIPAM homopolymers synthesised in cononsolvents

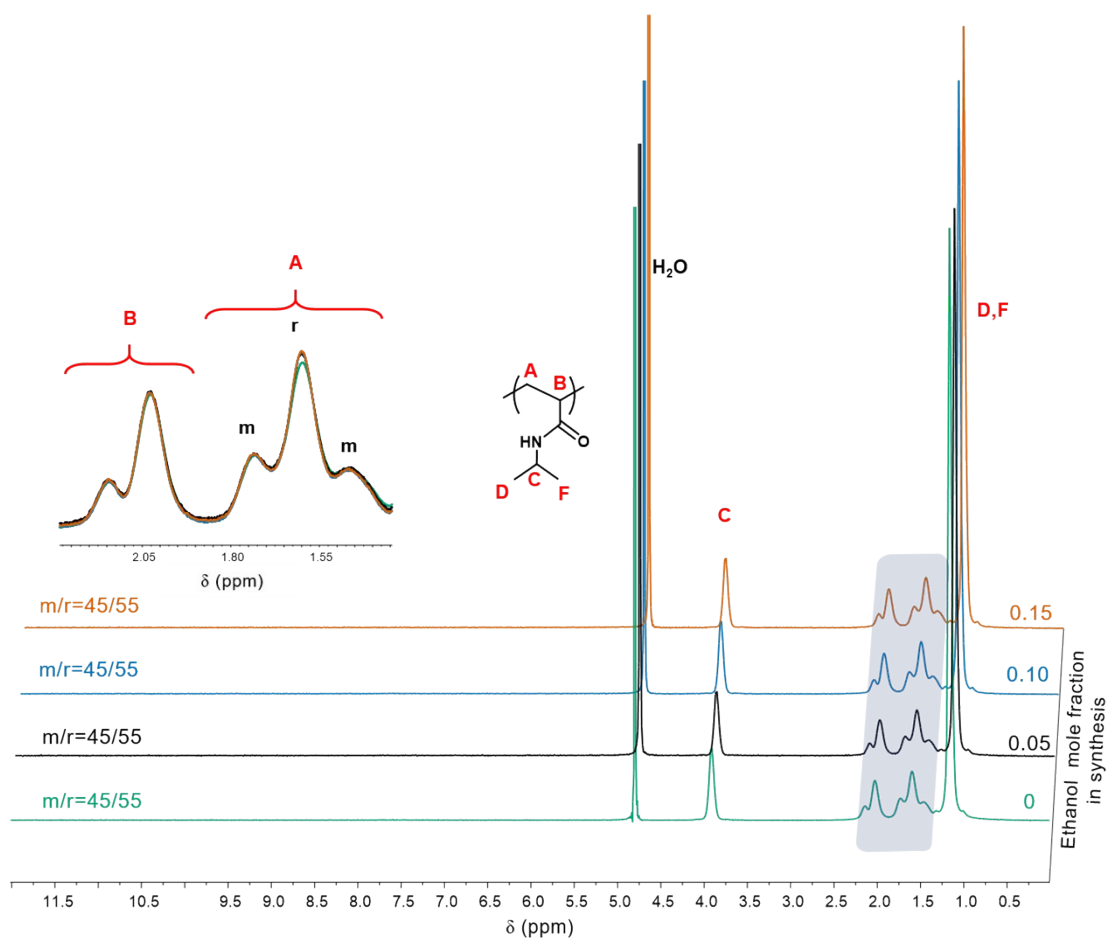


Figure S15. ^1H NMR spectra pNIPAM homopolymers synthesised by precipitation polymerisation in different water and water/EtOH mixtures. Spectra were recorded in D_2O .

Notes and references

1. A. L. Navarro-Verdugo, F. M. Goycoolea, G. Romero-Meléndez, I. Higuera-Ciapara and W. Argüelles-Monal, *Soft Matter*, 2011, **7**, 5847-5853.
2. S. Bandyopadhyay, A. Sharma, M. A. Ashfaq Alvi, R. Raju and W. R. Glomm, *RSC Advances*, 2017, **7**, 53192-53202.